16TH EUROPEAN CONFERENCE ON EARTHQUAKE ENGINEERING THESSALONIKI 18 - 21 JUNE 2018

ANALYTICAL FRAGILITY EMBODIED IN ON-SITE EARLY WARNING SYSTEM FOR INDUCED SEISMICITY

Konstantinos G. MEGALOOIKONOMOU[1], Stefano PAROLAI[2], Massimiliano PITTORE[3]

ABSTRACT

Earthquakes, despite being a mostly natural phenomenon, may also be induced by a wide range of anthropogenic activities such as mining, fluid injection and extraction, and hydraulic fracturing. In recent years, the occurrence of induced seismicity and its potential impact on the built environment have heightened both public concern and regulatory scrutiny, motivating the need for a framework for the management of induced seismicity. Earthquake early warning systems, coupled with non-standard monitoring approaches, provide valuable tools for mitigating the risk associated with earthquakes. These solutions might include the use of advanced sensors and the implementation of performance-based on-site early warning and rapid response systems for infrastructure, as well as monitoring the structural response of buildings and infrastructure in real time. Such technical solutions can be further used for validating damage forecasts determined by probabilistic approaches.
The goal of this study is to establish a monitoring and early warning system for induced seismicity. For this purpose, it is necessary to integrate analytical fragility curves in real time. These fragility curves can be derived by simplified vulnerability models that require input obtained from advanced exposure-monitoring techniques. Considering the case of induced seismicity, this also requires the expected damage to refer to non-structural components. Hence, the derived fragility curves are based on the non-structural damage criteria of typical residences. We therefore present a new approach for defining analytical fragility curves of traditional or historic masonry structures, which occur in large numbers near the geothermal platforms considered in this work.

Keywords: Non-standard monitoring; On-site early warning system; Fragility curve; Non-structural components; Induced seismicity

1. INTRODUCTION

Earthquakes are mostly natural phenomena that threaten millions of people worldwide. However, they may also be induced, or triggered, by a wide range of anthropogenic activities, such as mining, fluid injection and extraction, and hydraulic fracturing. Earthquake triggering refers to cases where seismogenic areas already close to failure are affected by industrial activities that, despite being relatively small, can perturb this critical state enough to initiate the rupture process. Such earthquakes may reach relatively high magnitude and are potentially dangerous. Induced earthquakes, which are much more common, refer to minor events directly caused by the change in stress and strain in the Earth's crust associated with the industrial activity. These events are usually characterized by small magnitudes, and therefore are mostly associated with non-structural damage to buildings and infrastructure. However, such damage may result in non-negligible economic losses and occasionally in the partial or total disruption of activities, causing additional losses. Furthermore, the occurrence of induced seismicity is largely uncorrelated with historical seismicity, and this represents an additional uncertainty factor and further reason for concern. Indeed, in recent years, the occurrence of induced

[1]Research Engineer, Centre for Early Warning Systems, GFZ German Research Centre for Geosciences, Potsdam, Germany, kmegal@gfz-potsdam.de
[2]Professor, Centre for Early Warning Systems, GFZ German Research Centre for Geosciences, Potsdam, Germany, parolai@gfz-potsdam.de
[3]Senior Researcher, Centre for Early Warning Systems, GFZ German Research Centre for Geosciences, Potsdam, Germany, pittore@gfz-potsdam.de

seismicity and its impact on the built environment have heightened both public concern and regulatory scrutiny, motivating the need for structured approaches to the assessment and managing of induced seismicity (Bommer et al. 2015). Efforts to develop systems to enable the control of seismicity have not yet resulted in solutions that can be applied with confidence in most cases. The more rational approach proposed nowadays is based on applying the same risk assessment and mitigation measures that are applied for the case of natural seismicity. This framework allows informed decision-making regarding the conduct of anthropogenic activities that may cause earthquakes. However, because of the specific characteristics of induced earthquakes — which may occur in regions with little or no natural seismicity — the procedures used in standard earthquake engineering need adaptation and modification for their application to induced seismicity.

Present structural design is concerned with life protection and collapse prevention of a structure. Over time, advances in structural engineering have created a large base of expertise that has substantially contributed to solving this problem. As a result, structures built with current methods are generally able to withstand expected seismic activity and maintain their structural integrity. However, although a building remains structurally sound, it can be rendered unusable due to damage to its non-structural components. Additionally, the majority of the value of some specific buildings and infrastructure lies in their non-structural components. For instance, it has been shown that non-structural components account for 82%, 87% and 92% of building costs for offices, hotels and hospital buildings, respectively (Taghavi and Miranda, 2003). Therefore, although structural damage is avoided, building owners may still be burdened with high expenses due to the need to repair and replace non-structural components.

In this paper the focus will be on the rapid and efficient modeling of an urban area from the point of view of the exposure (characterization of the number and structural features of the building stock) and of the vulnerability (considering only the possible damage to non-structural components). In particular, the aim of this study is to review the existing protocols for evaluating the fragility of non-structural components, and to propose new fragility curves for typical building types that have been developed for the seismic demands generally imposed upon linear and slightly non-linear systems of single and multiple degrees of freedom, which is the case for the effects of induced seismicity.

2. EXPOSURE AND VULNERABILITY MODEL

2.1 Exposure Model

In order to achieve the goal of limiting the consequences of induced seismic risk in real time, the exposure and the vulnerability models for the region under consideration should be defined. Regarding exposure models, coupling remote sensing and in-situ images can be optimized over broad areas for the characterization of the built environment (Pittore et al., 2012). The latter approach is feasible through the so-called Remote Rapid Visual Scanning Platform (RRVS) (Fig. 1). Through this platform, the Global Earthquake Model (GEM) Building Taxonomy can be employed (Pagani et al., 2014). This taxonomy is a standardized building and structural classification scheme used to categorize buildings in the same manner across the globe. It features 13 building ‘attributes’ ranging from what the building is used for (occupancy) to roof and wall material. These characteristics are crucial to not only understanding the performance of a building in case an earthquake strikes, but also to obtain an overview of the types of buildings exposed to seismic risk in a given area. It is a very comprehensive classification scheme, able to capture all (or at least most) different building types that exist around the globe. In addition, it is accompanied by tools that allow one to easily work with the building taxonomy. It is currently being used as a basis for the global exposure database and the global consequences database (Pagani et al., 2014).

Figure 1. Remote Rapid Visual Scanning.

2.2 Vulnerability Model

In loss estimation, one of the most important steps towards the evaluation of the total loss in buildings as a result of an earthquake is the "fragility curve", which represents the relationship between the structural response and the damage state of the building or structure of interest. In particular, a fragility curve provides a relationship between a structural response parameter, or Engineering Demand Parameter (EDP), and the probability of exceeding a specific state of damage. There are two EDPs that are well correlated to damage in buildings, and hence are particularly useful in performance-based earthquake engineering: a) Maximum interstory drift ratio (IDR) and b) Peak floor acceleration (PFA). Since almost all structural components are damaged as a result of structural deformation resulting from lateral deformation, the IDR provides a good measure of possible damage to a building´s structural elements. While a large portion of non-structural components are sensitive to IDR, some are vulnerable primarily as the result of inertial forces.
The Eurocode 8 does not define how demands on displacement-sensitive non-structural components should be estimated. However, the Eurocode 8 does specify (Cl.4.4.3.2) that for a seismic design intensity suitable for the damage limitation (serviceability) limit state, the peak story drift of the main structure (obtained from elastic analyses) should be limited to the following values, set as a function of the non-structural typology/detailing and represented by θ_{ns}, which is the limiting story drift ratio, equal to the relative inter-story displacement divided by the story height:

- for buildings having non-structural components fixed in a way so as not to interfere with structural deformations: $\theta_{ns} \leq 1.0\%$;
- for buildings having ductile non-structural components: $\theta_{ns} \leq 0.75\%$;
- for buildings having non-structural components, realized with brittle materials, attached to the structure: $\theta_{ns} \leq 0.5\%$.

One issue with the above drift limits for non-structural components is that the Eurocode 8 does not provide clear criteria for the classification of non-structural components as ductile, since a minimum required ductility capacity is not indicated. Nor it is clear why the drift should be limited to 1.0% if the non-structural components are detailed so as not to interfere with structural deformations, unless it is assumed that the fixings of such non-structural components would only need to allow the structure to move freely up to a drift demand of 1.0%. Nevertheless, the provision of the above limits does guarantee at least some consideration of deformation-sensitive non-structural components during the seismic design process.
According to D'Ayala and Meslem (2013), analytical fragility assessment methodologies are commonly based on two main components, namely the structural response-to-damage state functions, which are the product of two independent procedures, structural and damage analysis, and to which a certain level and type of uncertainty should be expected and accounted for by users when performing seismic risk assessments, and the ground motion intensity-to-structural response functions. Generally, most of the available methodologies used to develop analytical fragility curves include the following steps concerning uncertainty assessment: (1) identification of sources of uncertainty with regards to capacity, demand and damage thresholds definition, and (2) quantification of those uncertainties and their modeling when constructing fragility curves. With respect to the structural analysis phase,

uncertainties related to capacity and demand modeling are typically accounted for in the estimation of the building's performance (Maio and Tsionis, 2015). Non-structural components may contribute to the response behavior of the structure, as in the case of masonry infill walls in RC buildings, or be considered only in loss estimation modeling, in case they represent a significant proportion of the building's construction cost. There are different options available for the choice of mathematical modeling and type of analysis for structural assessment. Uncertainties related to these models are directly dependent on the level of complexity desired to conduct the fragility assessment. Even though single-degree-of-freedom (SDoF) models are not the most accurate, the simplification to an equivalent SDoF system (ESDOF) is widely used when computing the performance point and damage state of a structure in a number of methodologies for the determination of fragility curves.

3. PROPOSED METHODOLOGY FOR ANALYTICAL FRAGILITY CURVES

In order to adopt damage forecasts (performance) determined by probabilistic approaches, suitable fragility curves are necessary. Based on the performance level, an alert is designated according to pre-defined thresholds for acceptable levels of motion. Therefore, it is important to incorporate the fragility in an already developed on-site early warning and rapid damage forecasting system (Bindi et al., 2016) (Fig. 2). The exposure estimation dictates that traditional or historical masonry structures occur in large numbers near the geothermal platforms in remote and less populated areas like in the area of geothermal platforms in Alsace region in France. Two simple performance assessment models (Vamvatsikos et al., 2015, Kouris et al., 2014) are adopted in order to address the need for preliminary assessment tools for these classes of structures. The objective is to be able to rapidly identify buildings and their non-structural components that are at greater risk in the event of an induced earthquake.

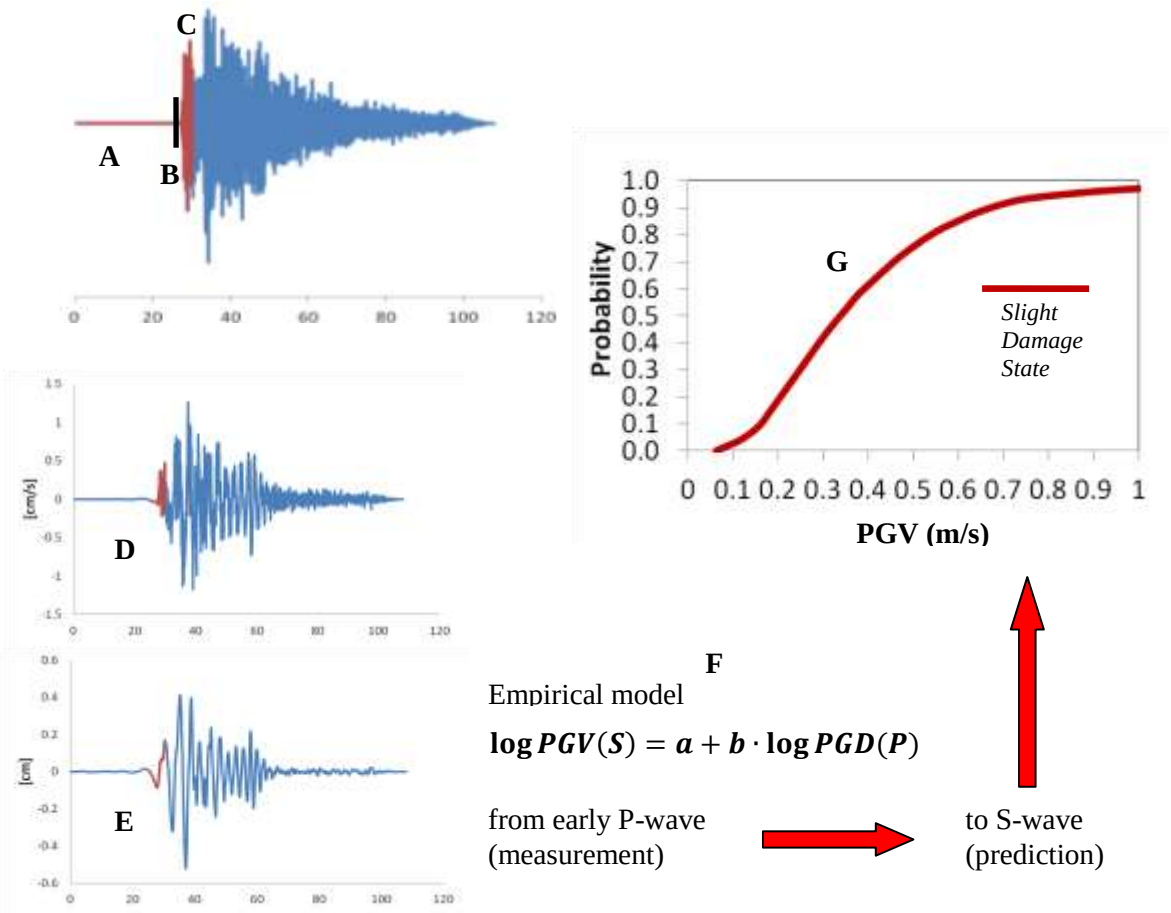

Figure 2. The developed on-site early warning system **A:** Real-time strong-motion acquisition; **B:** trigger based on short-time over long-time averages; **C:** estimation of strong motion parameters; **D:** estimation of parameters over velocity integrated signal; **E:** estimation of parameters over displacement integrated signal; **F:** prediction of PGV for S-waves using the PGD over P-waves; **G:** the fragility curves of the building.

3.1 Unreinforced Masonry Buildings (URM)

A significant difference between steel or concrete frames and URM structures exists, which complicates the direct extension of the established procedures to masonry buildings: frame structures are mostly lumped systems with stiff diaphragms, whereas URM buildings have distributed mass and stiffness with typically flexible diaphragms. The consequence of this is that the fundamental mode of vibration engages a disproportionately low fraction of the building mass well below the 75% cutoff value for mass participation which is a pre-requisite for the application of simple ESDOF-based methods. In order to solve this issue, the simplified procedure of Vamvatsikos et al. (2015) was adopted. It is formulated using an equivalent SDOF representation of the building's dynamic response. Both demand and supply in the critical locations of the structure needed for the evaluation of the acceptance criteria are established in closed-form in terms of deformation measures through the transformation of global response quantities to local measures. The transformation is based on the shape of the fundamental mode of spatial vibration of the structure, which is approximated by a three-dimensional shape function, derived consistently with the boundary conditions of the building. Acceptance criteria are established both in terms of deformation and strength indices. The model reproduces the global vibration characteristics while also employing a local deformation shape to allow the estimation of typical local failures (Fig. 3). An advantage of the procedure is that the end results are given in closed-form expressions, enabling the automation of the necessary calculations. The model's input involves only the key geometric characteristics of the considered box-shape masonry building (Fig. 3) as well as the wall thickness and shear strength and shear modulus of the URM wall, all of which are easy to determine. On the other hand, a disadvantage is that the assumptions made, in order to simplify the procedures, restrict the applicability of the shape-function used for the derivation of the ESDOF properties to simple box-type buildings with rectangular floor plans and flexible floor diaphragms. The application of such a model to irregular structures is not recommended.

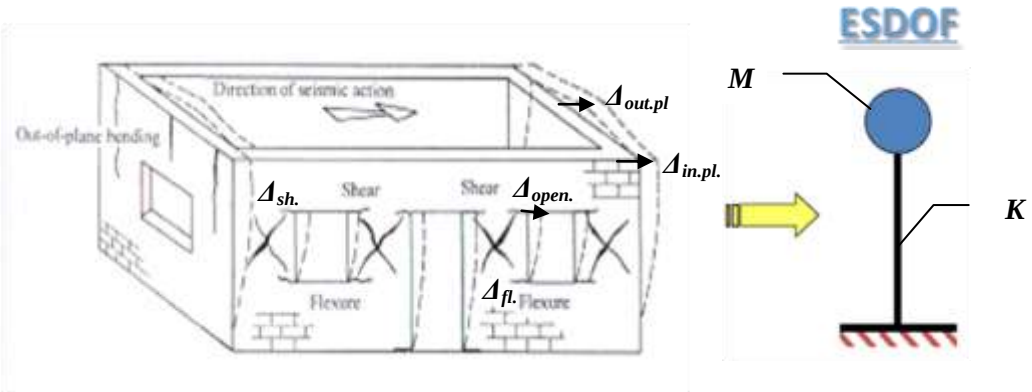

Figure 3. Equivalent Single Degree of Freedom (ESDOF) representation of typical box-shape unreinforced masonry (URM) building under earthquake-induced loading taking into account typical deformation components in the fundamental mode shape.

3.2 Timber-Framed Masonry Buildings (TFM)

TFM generally consists of masonry walls reinforced with timber elements, including horizontal and vertical elements, as well as X-type diagonal braces. Since the Bronze Age, TFM buildings were common in regions where moderate-to-strong earthquakes were frequent. There is ample historical evidence that the inclusion of timber elements into masonry walls is closely related to earthquake occurrence. Experimental and numerical evidence (Kouris et al., 2014) suggests that there is a key role for the diagonal braces and that there is also an early detachment of the masonry infills from the surrounding timber frame in the event of an earthquake. Another interesting conclusion is that diagonals in tension separate from the surrounding frame at very small levels of horizontal displacement. The authors of the above study suggested that the contribution of the infills should not be taken into account in analytical models and that the diagonals should be considered to contribute to

the lateral behavior of the TFM only in compression. Based on this conceptual approach, a macro-model was proposed (Kouris et al., 2014) (Fig. 4) where its input involves only the key geometric characteristics of the timber panels and the timber strength, all of which are relatively easy to determine. The model can then be used to assess the seismic behavior of TFM buildings in terms of their pushover curves and is deemed to be a useful tool for seismic vulnerability and risk analyses. Based on the resulting pushover curves and the macro-model, a shape-function is defined for the derivation of the ESDOF properties which is similar to URM buildings in order for the corresponding fragility curves to be derived in terms of peak ground acceleration (PGA) with the aid of structural analysis for a gradually increasing intensity (incremental dynamic analysis - IDA). The correlation of the PGA values of the recordings used in the IDA analysis with the corresponding PGV values follows the rule that for very flexible structures (very high fundamental periods) the relative velocity response spectrum of the used record tends to the peak ground velocity (PGV).

a) **b)**

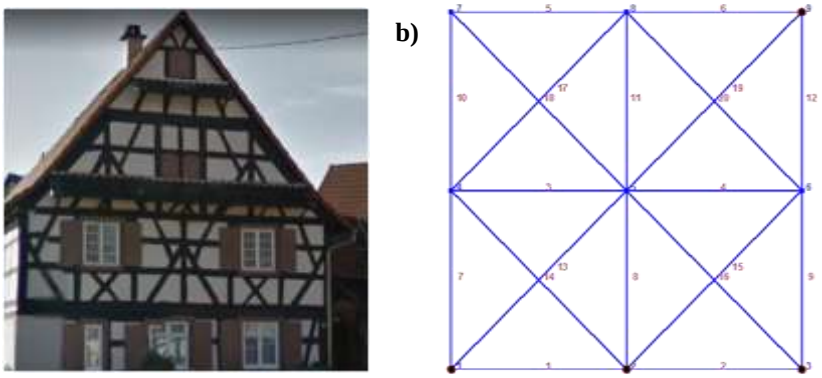

Figure 4. a) Example of a timber framed masonry building (TFM) b) TFM wall model with panels incorporating X-type diagonal braces.

4. ANALYTICAL FRAGILITIES FOR URM AND TFM BUILDINGS FOR INDUCED SEISMICITY DEMANDS

4.1 Induced Ground Motion Database

The web-based Pacific Earthquake Engineering Research Center (PEER) ground motion database provides tools for searching for, selecting, and downloading ground motion data. For the purpose of applying an incremental time history dynamic analysis (IDA) to the ESDOF models of the masonry buildings under consideration in this study, there is a need for realistic induced ground motion records.

Table 1. Earthquake events involving induced seismicity identified in the PEER database.

EQ -ID	EQ-ID Database	Year	Name	Location	M	Epicenter Latitude (deg)	Epicenter Longitude (deg)	Depth (km)
1	57	2010	Lincoln_2010-02-27	Lincoln OK	4.18	35.553	-96.752	4
2	66	2010	Slaughterville_2010-10-13	Slaughterville OK	4.36	35.202	-97.309	14
3	67	2010	Guy_2010-10-15	Guy AR	3.86	35.276	-92.322	5
4	73	2010	Arcadia_2010-11-24	Arcadia OK	3.96	35.627	-97.246	3
5	74	2010	BethelAcres_2010-12-12	Bethel Acres OK	3.23	35.392	-96.995	4
6	76	2010	Guy_2010-11-20	Guy AR	3.90	35.316	-92.317	5

7	80	2011	Greenbrier_2011-02-28	Greenbrier AR	4.68	35.265	-92.34	4
8	91	2011	Sparks_2011-11-06	Sparks OK	5.68	35.537	-96.747	9
9	92	2011	Comal_2011-10-20	Comal TX	4.71	28.81	-98.15	4

The PEER ground motion database was therefore examined to identify records of induced ground motion, of which 20 were selected. From the entire database, 9 induced earthquake events were selected, mainly located in the states of Oklahoma, Arkansas and Texas in the Unites States of America (Table 1). These earthquake events were shallow, with depths ranging from 3 to 14 km. Of the stations recording these events, a selection was made of the records that were closer to the epicenter, with an epicentral distances ranging between 5 and 55 km. The magnitude range of the selected events was between 3 and 5.5 (Fig. 5). The range of Peak Ground Acceleration (PGA) values can also be seen in Fig. 5.

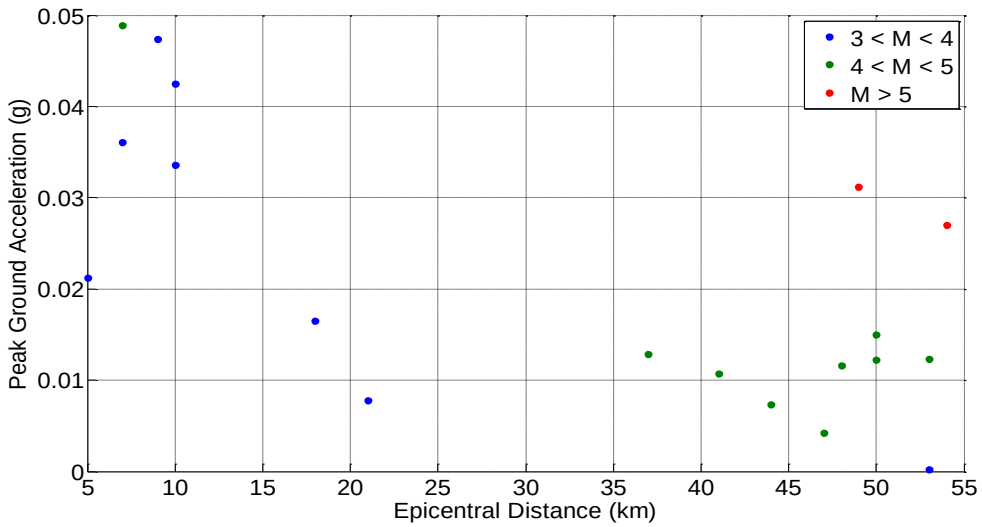

Figure 5. Peak Ground Acceleration (PGA) of the ground motions selected from the PEER seismicity database as a function of epicentral distance.

In Figs. 6, 7, and 8, the elastic response spectrums for some of the ground motion records under consideration in this study are presented. A comparison is also made with the type 2 elastic response spectrum of Eurocode 8 for earthquake magnitudes up to 5.5.

It can be seen that low-rise structures (that occur in large numbers near the geothermal platforms in remote and less populated areas) are mostly affected by this type of ground motion (attributed to the high-frequency content of the induced seismic waves from shallow earthquakes, having short duration and causing near-field damage). The maximum acceleration in some cases is comparable with that of Eurocode 8 elastic response spectrum for very soft soils.

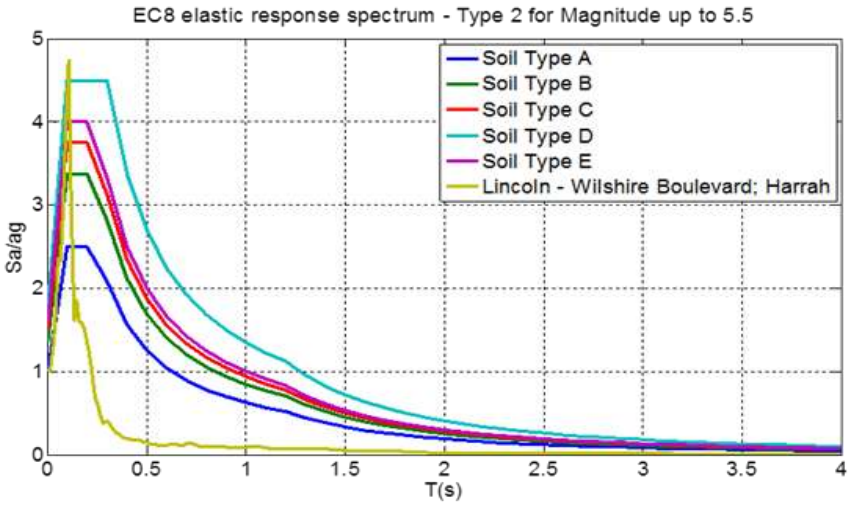

Figure 6. Elastic Response Spectrum of the induced-seismic ground motions obtained from the PEER database and their comparison with the Eurocode 8 Type 2 Elastic Response Spectrum for magnitudes up to 5.5.

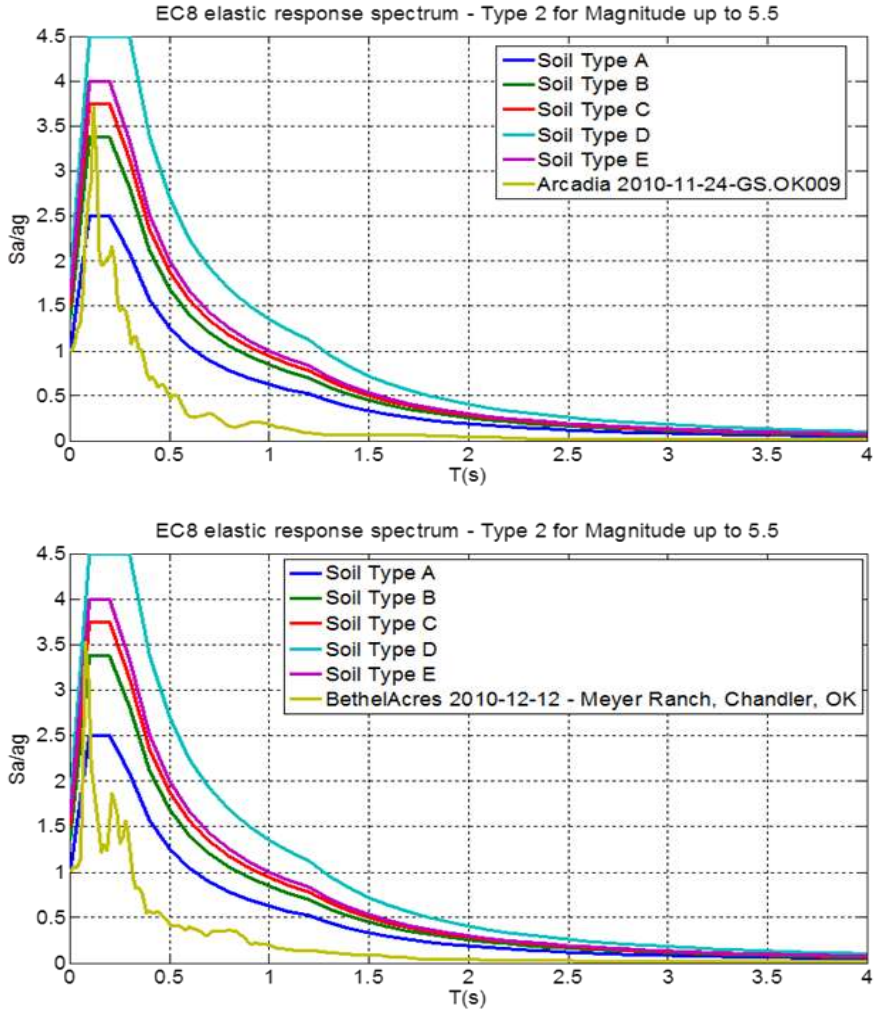

Figure 7. Elastic Response Spectrum of the induced seismic ground motions obtained from the PEER database and their comparison with the Eurocode 8 Type 2 Elastic Response Spectrum for magnitudes up to 5.5.

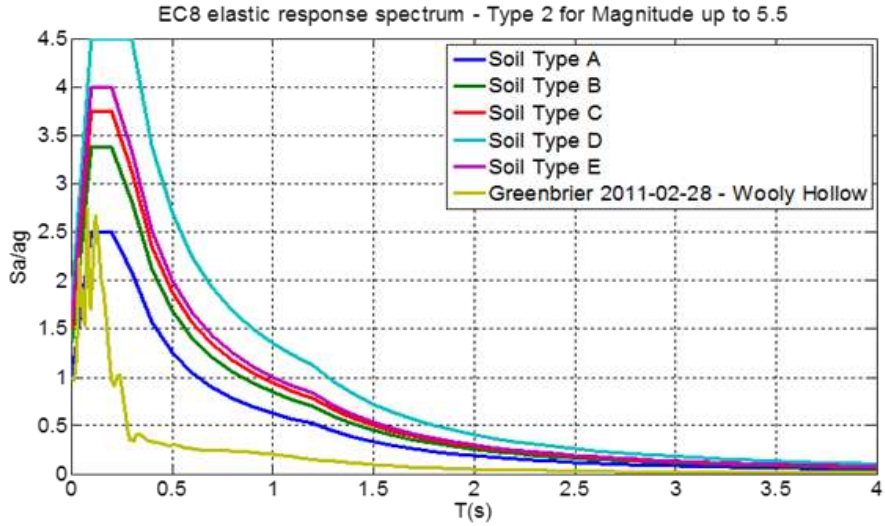

Figure 8. Elastic Response Spectrum of the induced seismic ground motions obtained from the PEER database and their comparison with the Eurocode 8 Type 2 Elastic Response Spectrum for magnitudes up to 5.5.

4.2 Unreinforced Masonry Buildings (URM)

The application of the methodology presented in this work for producing the fragility curves for URM buildings is demonstrated here on a simple unreinforced masonry model structure which was tested under simulated ground motions on a shake table by Bothara et al. (2010). The experimental fragility curve (available in the original publication) based on the experimental damage (measured drifts from incremental levels of shaking) is provided for comparison with those obtained by the analytical procedures. The building model was built at a scale of 1:2. The model had 0.11 m thick masonry walls, a rectangular floor plan of 2.88 m x 1.92 m, and was a two-storey structure with a first floor height of 1.34 m, a second floor height of 1.14 m, and a roof gable rising by 0.815 m. The structure was first tested using a suite of ground motions in the longitudinal direction, scaling them to PGA values in the range of 0.2-0.8 g. This testing was repeated by shaking the structure in the short direction of its plan. Due to the lack of stiff floor panels and connections, no diaphragm action was assumed.

Fig. 9 provides the analytical fragility curves for the pre-yielding damage state (which is the case for induced seismicity demands) with 0.1% drift limit. The curve was produced using incremental dynamic analysis IDA of the ESDOF of the above mentioned scaled URM building, employing the induced ground motions obtained from the PEER database previously presented and applied in the longitudinal and transverse building plan directions. It can be seen that the fragility curve produced by the elastic time history analysis in the transverse (weak) direction of the URM building is close to the experimental fragility curve obtained from the experimental data. In addition, the drift limit for damage to drift sensitive brittle non-structural components provided by the Eurocode 8 was also applied to the results of the IDA in the short building plan direction and the corresponding fragility curve is also provided. It is noteworthy that the roof tiles (drift-sensitive brittle non-structural components) of the experimental model that were not connected to the roof structure, scattered badly during the experiment and a few of them slid off the roof when subjected to a PGA of 0.5g. However, in real event, such tiles would slide off at much lower level of shaking. By applying the Eurocode 8 drift limit to this case, the corresponding fragility curve couldn't capture the PGA corresponding to the experimental failure of the roof tiles. The correct drift limit in this case for drift-sensitive brittle non-structural components should therefore be 0.1% or lower.

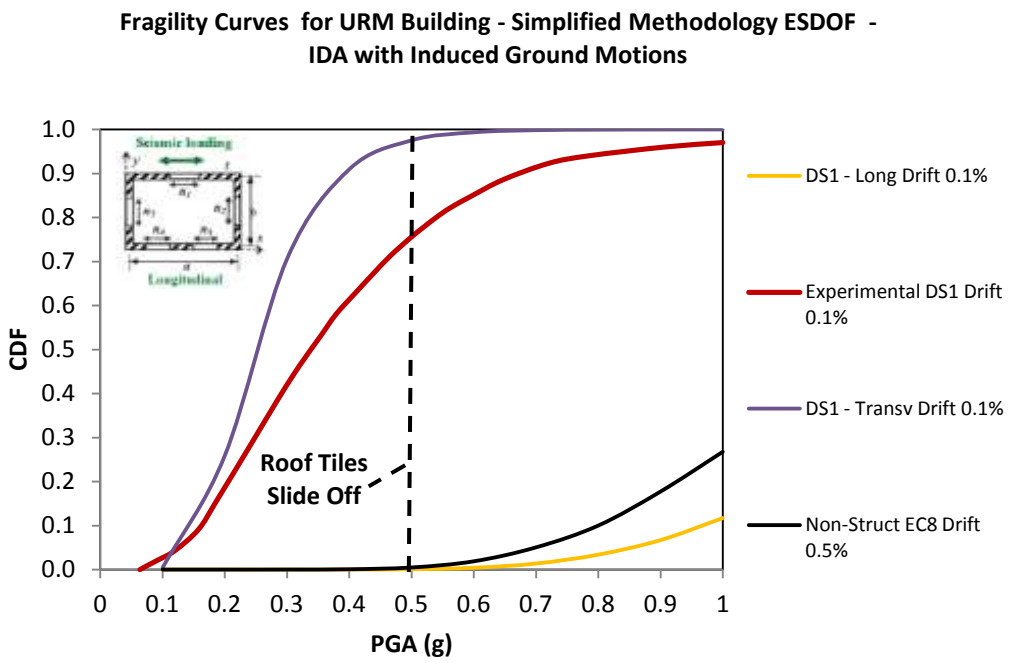

Figure 9. Analytical fragility curves for first damage state (pre-yielding damage state –DS1) for an Unreinforced Masonry Building (URM) tested experimentally in a shake table. Longitudinal (Long) and transversal (Transv) or short plan view directions of shaking are considered. The Eurocode 8 (EC8) drift limit for brittle non structural components is also applied. The vertical dashed line dictates the experimental PGA threshold over which detachment of the roof tiles of the URM building under study has been observed.

4.3 Timber-Framed Masonry Buildings (TFM)

In the case of TFM buildings, to the authors' best knowledge, there is only experimental evidence from the cyclic excitation of TFM walls and not shake table tests of a TFM building model. Therefore, the analytical procedure adopted here for the definition of the fragility curves of TFM buildings is validated through the non-linear static analysis of TFM walls. Based on the analytical model, a shape-function of the box-shaped TFM building is defined to derive the ESDOF properties in order for the corresponding fragility curves to be obtained in terms of PGA with the aid of IDA.

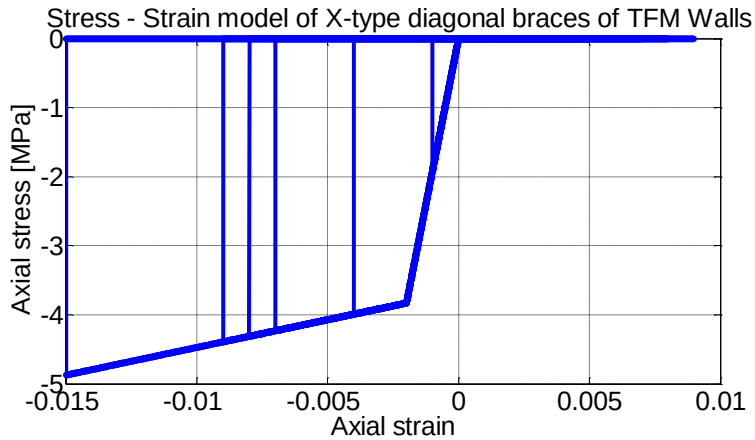

Figure 10. Stress – Strain material model of the non-linear truss elements representing X-type timber diagonal braces.

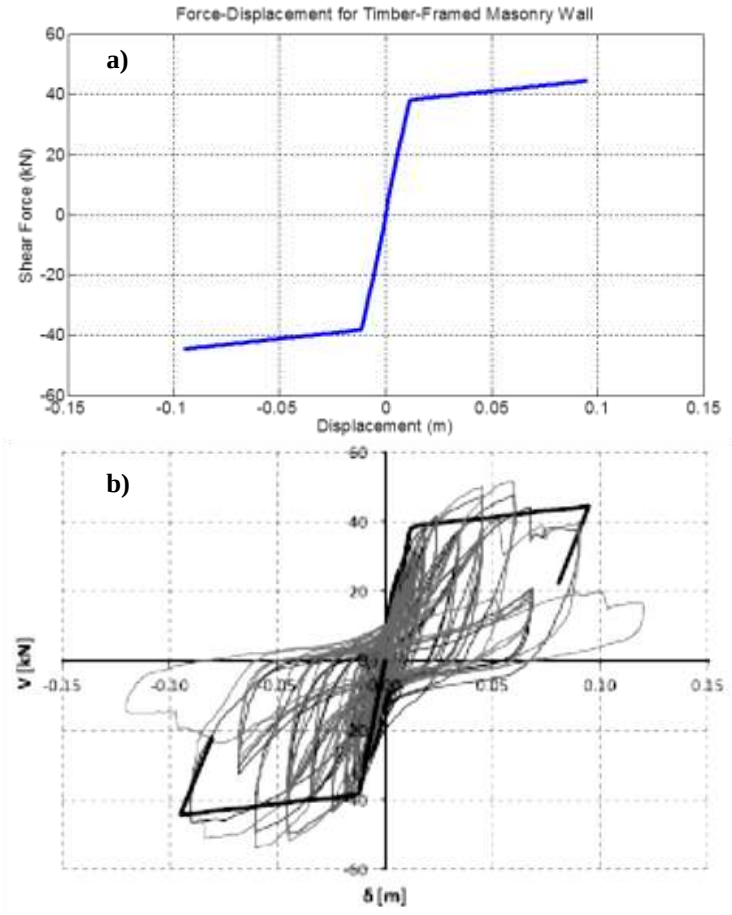

Figure 11. Comparison of the pushover curves from the methodology adopted by Kouris et al. (2014) (a) and the experimental results by Meireles et al. (2012) (b).

The macro model adopted by Kouris et al. (2014) involves the discretization of the building into individual timber-framed panels with equivalent truss model with elastic horizontal and vertical truss elements, but non-linear diagonal truss elements (Fig. 4b). The adopted empirical model is then used for defining the non-linear material constitutive law of non-linear truss elements representing the diagonal braces that contribute only in compression (Fig. 10). An example of the resulting pushover curve is given in Fig. 11 where the analytical capacity curve is compared with the experimental results by Meireles et al. (2012). It can be seen that there is good agreement between the numerical and experimental results, and therefore the empirical model of Kouris et al. (2012) is advisable for the definition of the analytical fragility curves through IDA. For the induced seismicity demands, only the pre-yielding damage state is of interest.

5. CONCLUSIONS

The ultimate objective of any effective program for the management of induced seismicity must be to limit the potential risk. It is therefore important to incorporate into an on-site early warning and rapid damage forecasting system the fragility curves that accurately describe the damage to non-structural components which often represent the majority of the cost of a building. Based on the proposed conceptual approach, the methodology followed considers the key geometric characteristics that are collected and represented in the exposure model. The adopted procedure can be used to assess the seismic behavior of masonry buildings and it is deemed to be a useful tool for seismic vulnerability and risk analyses. A shape-function is defined for the derivation of the ESDOF properties of URM and TFM buildings. In this way, the corresponding fragility curves are derived in terms of peak ground acceleration (PGA) with the aid of structural analysis for a gradually increasing intensity (incremental

dynamic analysis - IDA). This simplified model reproduces the global vibration characteristics while also employing a local deformation shape to allow the estimation of typical local failures. An advantage of the procedure is that it allows the automation of the necessary calculations in order to reliably extend the seismic vulnerability analysis to large inventories of buildings. Finally, the real-time performance-based on-site early warning and rapid response system for induced seismicity was introduced, incorporating these analytical fragility curves for non-structural components of masonry buildings. These curves have been developed for linear and slightly non-linear systems of single and multiple degrees of freedom for the range of intensities expected for induced seismicity.

6. ACKNOWLEDGMENTS

This work has been supported financially by the European Union funded project DESTRESS (http://www.destress-h2020.eu) (Work Package 3.4).

7. REFERENCES

Bindi D., Iervolino I., Parolai S. (2016) On-site structure-specific real-time risk assessment: perspectives from the REAKT project, *Bull. Earthq. Eng.*, 14(9): 2471-2493.

Bommer J. J., Crowley H., Pinho R. (2015). A risk-mitigation approach to the management of induced seismicity, *J. Seismol.* 19:623–646.

Bothara, J. K., Dhakal, R. P., Mander, J. B. (2010). Seismic performance of an unreinforced masonry building: An experimental Investigation. *Earthquake Engineering and Structural Dynamics*, 39:45–68.

CEN (2004) *Eurocode 8*: design of structures for earthquake resistance - Part I: general rules, seismic actions and rules for buildings. European Committee for Standardization (CEN). Brussels, Belgium.

D'Ayala D, Meslem A (2013) Sensitivity of analytical fragility functions to capacity-related parameters. *GEM Technical Report 2013-X*, GEM Foundation. Pavia, Italy.

Kouris L.A.S., Kappos A.J. (2014) A practice – oriented model for pushover analysis of a class of timber-framed masonry buildings, *Engineering Structures Journal*, Elsevier, 75: 489-506.

Maio R., Tsionis G (2015). Seismic fragility curves for the European building stock, *JRC Technical Report*, European Commission.

Meireles H, Bento R, Cattari S, Lagomarsino S. (2012). A hysteretic model for ''frontal'' walls in Pombalino buildings. *Bull. Earthq. Eng.* 10:1481–502.

Pagani, M., D. Monelli, G. Weatherill, L. Danciu, H. Crowley, V. Silva, P. Henshaw, Butler, L., Nastasi, M., Panzeri, L., Simionato, M., and Vigano, D. (2014). OpenQuake Engine: An Open Hazard (and Risk) Software for the Global Earthquake Model. *Seismological Research Letters* 85 (3):692–702.

PEER-NGA-East Database (2017). Pacific Earthquake Engineering Research Center, University of California, Berkeley, CA, (http://peer.berkeley.edu/ngaeast/).

Pittore M., Wieland M. (2012) Toward a rapid probabilistic seismic vulnerability assessment using satellite and ground-based remote sensing. *Natural Hazards*. 68(1):115-145

Taghavi, S., Miranda, E. (2003). Response Assessment of Nonstructural Building Elements, *PEER Report 2003/05*, University of California Berkeley.

Vamvatsikos D. , Pantazopoulou S. J. (2015) Development of a simplified mechanical model to estimate the seismic vulnerability of heritage unreinforced masonry buildings. *Journal of Earthquake Engineering*, Taylor & Fran, 20(2): 298-325.